



OPEN

The early heat loss evolution of Mars and their implications for internal and environmental history

SUBJECT AREAS:
INNER PLANETS
PLANETARY SCIENCE

Javier Ruiz

Departamento de Geodinámica, Facultad de Ciencias Geológicas, Universidad Complutense de Madrid, 28040 Madrid, Spain.

Received
30 August 2013
Accepted
20 February 2014
Published
11 March 2014Correspondence and
requests for materials
should be addressed to
J.R. (jaruiz@geo.ucm.
es)

The time around 3.7 Ga ago was an epoch when substantial changes in Mars occurred: a substantial decline in aqueous erosion/degradation of landscape features; a change from abundant phyllosilicate formation to abundant acidic and evaporitic mineralogy; a change from olivine-rich volcanism to olivine-pyroxene volcanism; and maybe the cessation of the martian dynamo. Here I show that Mars also experienced profound changes in its internal dynamics in the same approximate time, including a reduction of heat flow and a drastic increasing of lithosphere strength. The reduction of heat flow indicates a limited cooling (or even a heating-up) of the deep interior for post-3.7 Ga times. The drastic increasing of lithosphere strength indicates a cold lithosphere above the inefficiently cooled (or even heated) interior. All those changes experienced by Mars were most probably linked and suggest the existence of profound interrelations between interior dynamics and environmental evolution of this planet.

Paleo-heat flows based on determinations of lithospheric strength are useful for obtaining information on the thermal evolution of a planetary body^{1–3}. So, Ruiz et al.³ used paleo-heat flow estimates for 22 martian regions of different periods and geological contexts, derived from the effective elastic thickness of the lithosphere or from faulting depth beneath large thrust faults, to constrain the thermal history of Mars. The results obtained by these authors suggest that Mars has been losing less heat than predicted from most thermal history models^{4–6}. The martian mantle could even have been heating-up during a substantial portion of its evolutionary history.

An interior of Mars inefficiently cooled is, as pointed out by Ruiz et al.³, consistent with several independent geophysical and geological observations: the present-day existence of a (at least partly) fluid core⁷, and the simultaneous absence of an endogenic magnetic field⁸, are in agreement with high mantle temperatures reducing core cooling, and weakening or suppressing core convection; a lower amount of global contraction since the Early Noachian than expected from thermal history models, as deduced from thrust faults recorded on the surface⁹, because lack of mantle cooling limits the thermal contraction that can drive surface contraction; the evidence for recent extensive volcanism¹⁰ also suggest the retention of a substantial amount of internal heat. On the other hand, a limited interior cooling would be in agreement with a recent thermal history modeling¹¹, which take into account phase transitions and compositional changes due to mantle melting.

I add here that recent petrologic modeling^{12–14} of magma production finds higher potential mantle temperature for magmas originating shergottite meteorites (which typically have ages younger than 0.6 Ga) than for magmas originating Gusev and Meridiani basaltic rocks, which are Noachian in age. (This period corresponds to ages older than 3.7 Ga, and was followed by the Hesperian; e.g., Ref. 15) Shergottite meteorites could have originated in a hot-plume environment, and therefore be not representative of the average mantle, but a long-term heating-up mantle would be a solution to the problem of the high-temperature shergottites.

The relatively low paleo-heat flows deduced for Mars from lithospheric strength are mostly related to post-Noachian times³. Otherwise, most of paleo-heat flows obtained for Noachian times are high or lower limits, and in the second case the heat flows could also be high; this would be consistent with an early time of intense interior cooling. In this work I investigate the key question of timing the change from high heat flows to comparatively low heat flows, through both (1) the comparison between radioactive heat production and surface heat flow as a function of time, and (2) the temporal pattern of lithospheric strength evolution, which relates to the thermal evolution of the lithosphere. I then compare this timing with other major events in the martian history, and discuss the implications of the heat loss history of Mars for the evolution of mantle temperature, core dynamo, and climate of this planet.



Results

The evolution of the interior heat budget as constrained by paleo-heat flows. The Urey ratio (Ur), the ratio between the total radioactive heat production and the total heat loss through the surface of a planetary body, constitutes an excellent means to visualize the internal heat budget of a planetary body. Thus, information on both paleo-heat flows and global planetary composition can be used to constrain the evolution of the Urey ratio, and hence the thermal evolution of a planetary body.

I have calculated Urey ratios (or more exactly, paleo-Urey ratios) for Mars from paleo-heat flows derived from lithospheric strength and the total radioactive heat production (function of age) derived from the global compositional model of Wänke and Dreibus¹⁶. The Urey ratio values were calculated extrapolating heat flows obtained for a given region to the entire planet. It is obvious that those “local” paleo-heat flows are not necessarily representative of globally average values, but so-derived “equivalent” Ur values are certainly informative, as I show below. For $Ur > 1$ ($Ur < 1$) the interior, as an average, is heating-up (cooling-down). Thus, for a given feature and time I have selected the upper limit surface heat flow (Figure 1), which in turn gives a lower limit for Ur , being therefore the less favorable cases for a limited cooling or a heating-up of the martian interior, and making more robust my conclusions.

The used paleo-heat flows (Figure 1) are mostly based on the upper limits obtained by Ruiz et al.³, although I have expanded the calculations for Olympus Mons, Arsia Mons, and Elysium rise in order to take into account an higher age range for the time of loading of the lithosphere supporting these volcanic edifices. Previous work^{2,3} considered the time of loading of Olympus Mons, and Tharsis Montes to be generally Amazonian (i.e., younger than ~ 3 Ga), in accordance with the ages of surface-covering lavas. However, crater counts of volcano flanks suggest that the main edifice, or at least a substantial portion, of those volcanoes was already emplaced around 3.5–3.6 (Ref. 17), and therefore, the time of loading could have been mostly Hesperian¹⁸. Similarly, flexure modeling and crater counts

suggest that most of Olympus Mons would have constructed between 3.67 and 2.54 Ga (Ref. 19).

Figure 2 shows lower limit estimates of Urey ratio for Mars as a function of time. Curve lengths indicate uncertainty related to feature age, not temporal evolution. For clarity, I have simplified the representation to show only the lower Urey ratio value obtained for a given region. Heat flows for post-Noachian volcanic regions would be consistent with $Ur < 1$ if these regions were loaded in the Amazonian, although volcanic areas are expected to be associated with heat flows higher than planetary averages. However, as stated above, refined crater counts suggest relatively early ages for the emplacement of Elysium and Tharsis volcanoes¹⁷, and therefore a Hesperian age for the associated loading¹⁸, and hence $Ur > 1$ values are favored from these features for the Hesperian. Moreover, all post-Noachian non-volcanic regions give Ur values higher than, or close to, 1; similarly, the present-day upper limit heat flow derived for the North Pole region is slightly above the present-day heat production, consistent with an upper limit Ur close to 1 (Ref. 3; see also Figure 1). The conclusion of a limited interior cooling seems therefore inescapable for post-Noachian times; moreover, the case for an interior heating-up is robust, at least during the Hesperian.

For the Noachian the situation is unclear, because many heat flow estimates for the Noachian southern highlands are lower limits^{2,3} (and so they are not shown in Figure 1), based on upper limit effective elastic thicknesses. Therefore a very high surface heat flow, and hence a very low Urey ratio, cannot be ruled out for the time when the large-scale topography of these regions was formed (for illustrating this, an Urey ratio close to zero for the southern highlands has been represented in Figure 2). Thus, most of the heat flows derived for Noachian terrains could be consistent with $Ur < 1$ and a substantial interior cooling. Relatively low heat flows deduced from the depth of large thrust faults at Amenthes Rupes and Warrego rise could suggest a highly variable heat loss across the martian surface in the Noachian, although the age of these thrust faults would be, respectively, between 3.6 and 3.8 Ga and between 3.7 and 4.0 Ga (Refs. 20, 21), whereas the

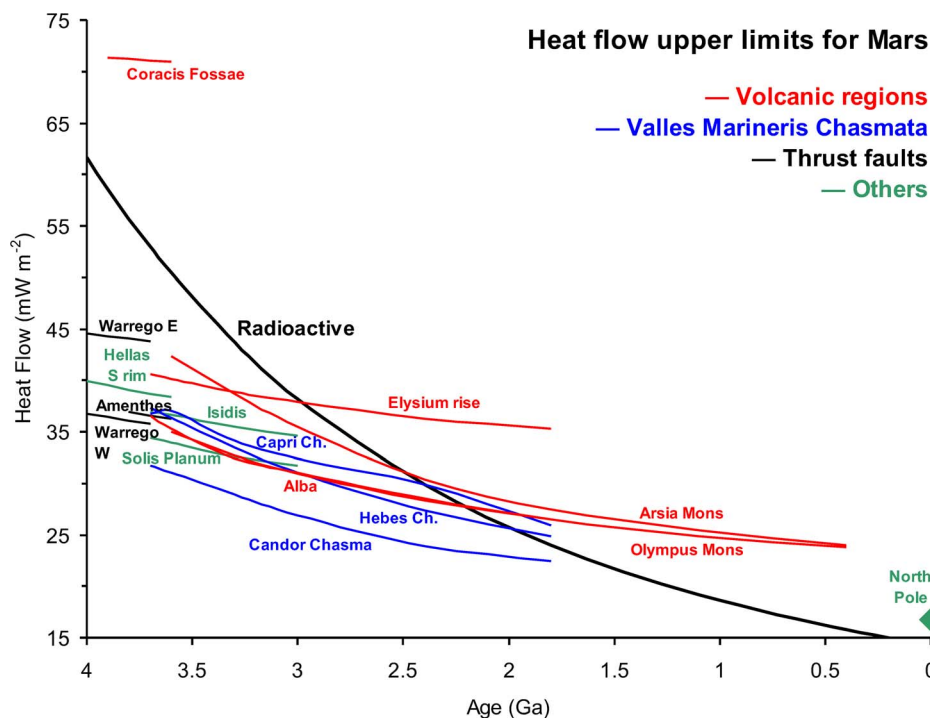


Figure 1 | Surface heat flow upper limits for several regions and times of Mars, indicating the geological category of the respective features. Curve lengths indicate uncertainty related to loading/deformation age (and hence to radioactive heating in the lithosphere), not temporal evolution. Most of heat flows shown in this figure are from Ruiz et al.³, although the calculations have been expanded in order to account for an higher age range for the time of loading of the lithosphere supporting Olympus Mons, Arsia Mons, and Elysium rise (see text for details).

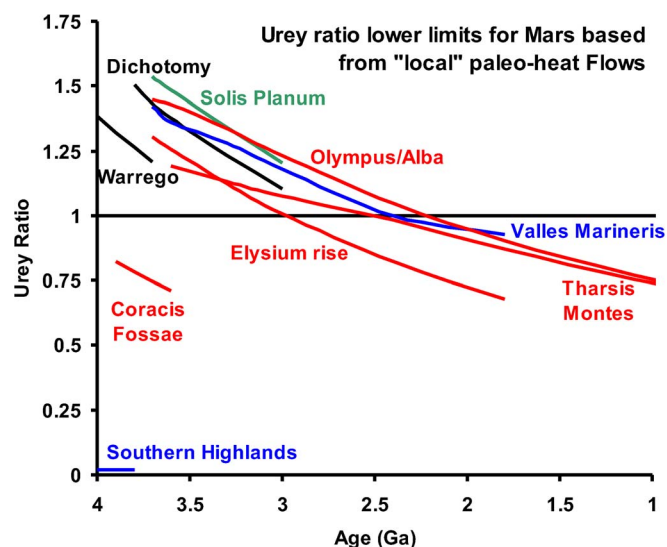


Figure 2 | Lower limits for the Urey ratio (U_r) calculated from Paleo-heat flow values in Figure 1. Curve lengths indicate uncertainty related to loading/deformation age (and hence to radioactive heating in the lithosphere), not temporal evolution. For geographically close regions only a composite curve including the Urey ratio lower limit for a given time is shown; for example, the curve labelled Dichotomy includes values from Amethes Rupes and Isidis Planitia. An U_r lower limit close to zero for the Southern highlands (including Amethes highlands, NE Arabia Terra, Noachis Terra, Terra Cimmeria and Hellas Basin) has been also represented, because there are available paleo-heat flows lower limits, but not upper limits, for these regions^{2,3}.

southern highlands would be older than 3.8 Ga (see Table 1). The heat flows lower limits derived for the southern highlands could therefore correspond to times earlier than those represented by the thrust faults, and so we cannot currently discard a transition from high heat flows (and $U_r < 1$) to low heat flows (consistent with U_r higher than, or close to, 1) occurred some time before the end of this period, maybe around 3.8 Ga.

The evolution of lithospheric strength and thickness. The effective elastic thickness, T_e , is related to the strength of the lithosphere, integrating contributions from brittle and ductile layers and from elastic cores of the lithosphere (for a review see Ref. 22); when considering curvature due to lithospheric flexure, T_e can in fact be used as a measure of the total strength of the lithosphere. Mantle rocks are stronger than crustal rocks, but under higher temperatures, which in turn reduces their strength. For a sufficiently high heat flow the upper mantle does not contribute to T_e , and the lithosphere is thin and restricted to the crust. Conversely, if the heat flow is sufficiently low, the upper mantle is cold and strong, and contributes to the strength of the lithosphere, and hence to the effective elastic thickness, which is therefore higher. Thus, the evolution of the effective elastic thickness is very interesting as an indicator of the evolution of the thermal state, strength and mechanical behaviour of the lithosphere.

Table 1 shows a summary of effective elastic thickness values derived for martian terrains loaded in different times, compiled from several works (see Methods Section). Much of these T_e estimates are not adequate for performing well-constrained heat flow calculations (and for that reason heat flow values for the respective regions are not shown in Figure 1), because curvatures of the equivalent elastic layer were not derived, but they are interesting as a way to constrain the evolution of lithosphere strength, and hence the thermal history of Mars. Figure 3 shows effective elastic thickness values derived for martian terrains loaded (or that could have been loaded) in Noachian

or Hesperian times, as a function of the age derived from model-ages based in crater counts; for representation clarity, Figure 3 shows only the central value of the range of T_e for each feature.

T_e estimates proposed for Noachian times are lower than 25 km, which are low relative to values obtained for post-Noachian terrains, suggesting a comparatively high heat flow in that time. Regions loaded (or that could have been loaded) in Late Noachian or Early Hesperian times (corresponding to an age range between 3.8 and 3.6 Ga; Ref. 15), show a wide dispersion of T_e values, generally higher than for Noachian, and very high values appear. Otherwise, most of T_e values for Hesperian or Amazonian times are higher than ~40–50 km, implying low heat flow and a significant contribution of the upper mantle to the strength of the lithosphere. Indeed, as indicated above, if the uppermost mantle is sufficiently cold then it contributes to the strength and effective elastic thickness of the lithosphere, and this results in an increased T_e (e.g., Refs. 22,23). Moreover, if such a strong mantle lithosphere is welded to the crust (which occurs if the strength at the crust base is sufficiently high) then there is a drastic increasing of T_e with respect to the case with mechanically decoupled crust and mantle lithosphere^{23,24}.

Thus, the transition from low to high values of T_e occurred around the Noachian/Hesperian boundary, with a substantial increasing of T_e after 3.6–3.7 Ga. This transition is related to a substantial contribution of the mantle to the strength of the lithosphere, and maybe to crust-mantle lithosphere welding. Thermal evolution models^{23,24} have shown that a local substantial increasing in T_e does not necessarily require a change in heat flow decline; but the timing of T_e increasing can largely vary from a region to another as a consequence of differences in the local lithospheric thermal regime²³ (including variations in other local factors, such as curvature and crustal thickness, should make more important this effect), but Figure 3 shows a general increase in T_e is a relatively narrow temporal window. The timing for this dramatic lithospheric strength increasing is similar to that for the inferred starting of $U_r > 1$ values. (Under appropriate conditions a reduction of heat flow may simultaneously produce interior heating of the convective mantle and cooling and thickening of the lithosphere³.) In any case, this lithospheric strength increasing was probably not simpler, since the dispersion of T_e values for Late Noachian or Early Hesperian times; this is not surprising, as lithosphere strength depends, among other factors, on crustal thickness and curvature^{3,22}.

On the other hand, the frequently stated increasing of T_e with age through the martian history (e.g., Ref. 25) is not evident after Early Hesperian, but uncertainty in loading time for most of T_e estimates for post-Noachian terrains preclude us of obtaining a definitive conclusion with respect to this point. The effective elastic lithosphere loaded by the north polar cap, a nearly current structure, has been inferred to be thicker than 300 km (Ref. 26), but the case for the lithosphere under the south polar cap, whose present-day effective elastic thickness could be as low as 110 km, is more poorly constrained²⁷.

Discussion

The time around the Noachian/Hesperian boundary was an epoch when substantial changes in Mars occurred (Figure 4): there is abundant evidence for a substantial decline in aqueous erosion/degradation of landscape features^{28–30}, indicating a reduction of the amount or lifespan of liquid water on the surface; a change from abundant phyllosilicate formation to abundant acidic and evaporitic mineralogy occurred some time previously to the end of the Noachian, indicating a transition from wetter to drier environmental conditions^{31,32}; a change from olivine-rich to olivine-pyroxene volcanism, indicating a modification in magma composition that could be due to a reduction of mantle temperature^{33,34} or to melts formed under higher pressure, and therefore from a deeper magma source below a thicker lithosphere³⁴. Similarly, recent careful examinations



Table 1 | Effective elastic thickness of the lithosphere derived for several martian terrains

Feature ^a	Surface age (Periods) ^b	Surface age (Ga) ^b	T_e (km) ^c
North Pole	Current	Current	>300
South Pole	Current	Current	>110
Valles Marineris (1)	H-A	3.6–1.8	≥60
Alba Patera (2)	H-A	<3.5	43–65
Arsia Mons (3)	H (or A)	~3.5 (or lower)	20–35
Pavonis Mons (4)	H (or A)	~3.6 (or lower)	50–100
Ascraeus Mons (5)	H (or A)	~3.6 (or lower)	50–80
Olympus Mons (6)	H-A	3.7 to 2.5	>70
Elysium rise (7)	H	3.7–3.0	36–45
Syrtis Major (8)	H	3.7–3.0	10–15
Solis Planum (9)	H	3.7–3.0	24–37
Isidis Planitia	H	3.7–3.0	100–180
Amenthes, dichotomy (10)	N-H	3.8–3.6	15–35
Aeolis region (11)	N-H	3.8–3.6	10–15
Hellas S rim (12)	N-H	3.8–3.6	20–120
Hellas W rim (13)	N-H	3.8–3.6	<20
Amazonis Planitia (14)	N-H	3.7–3.6	<45
Acidalia Planitia (15)	N-H	>3.6	13–30
Arcadia Planitia (16)	N-H	>3.6	<23
Thaumasia Highlands (17)	N-H	3.8–3.6	19–23
Tyrrhena Patera (18)	N-H	3.9–3.3	<28
Coracis Fossae (19)	N-H	3.9–3.5	10–13
Acheron Fossae (20)	N-H	3.9–3.6	9–11
Amenthes, highlands (21)	N	>3.8	<25
NE Arabia Terra (22)	N	>3.8	<16
Noachis Terra (23)	N	>3.8	<12
Terra Cimmeria (24)	N	>3.8	<12
Hellas Basin (25)	N	4.1–3.9	<13

^aThe numbered features refer to those represented in Figure 3.

^bAge relations based on Refs. 2, 17, 20, 49, 51, 56–60.

^cFor determination of T_e ranges see Methods Sections.

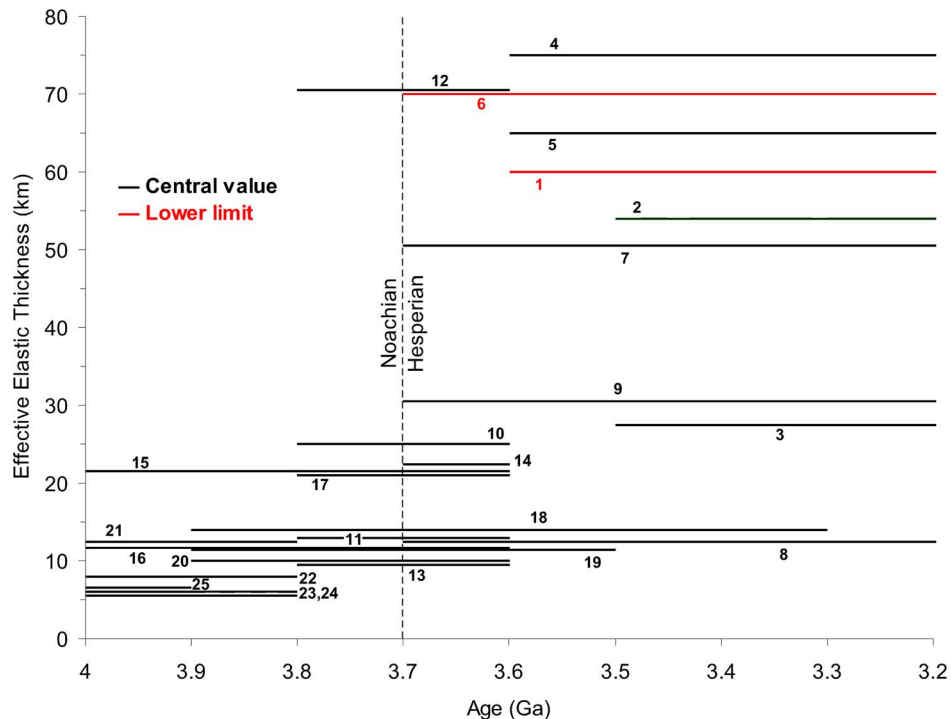


Figure 3 | Effective elastic thickness of the lithosphere (T_e) for martian terrains loaded (or that could have been loaded) in Noachian or Hesperian times, as a function of age. Numbers referring to given geological features are as in Table 1. For clarity, for a given feature only the central T_e value of the range in Table 1 is shown. Line lengths indicate uncertainty related to loading age.

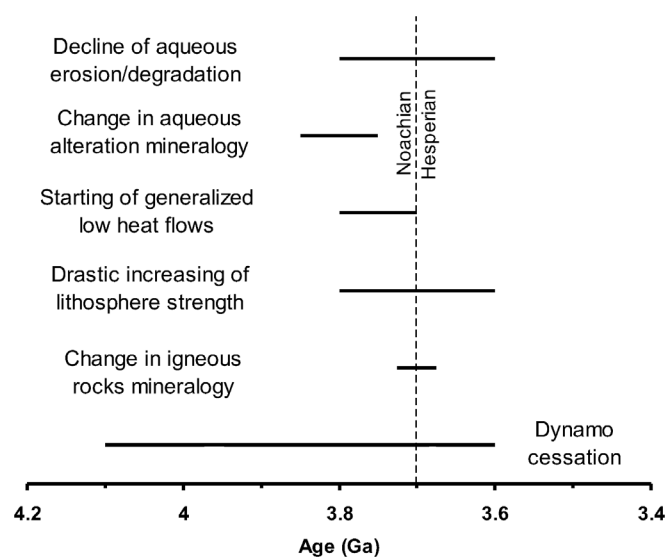


Figure 4 | Time range for several important changes that occurred in Mars around or close to the Noachian/Hesperian boundary.

of the age of isolated magnetic anomalies and of the size-age pattern of magnetization of impact basins suggest a cessation of the martian dynamo around 3.6–3.8 Ga (Refs. 35, 36); the usual vision of the martian dynamo ceasing around 4.0–4.1 Ga, based on the demagnetization (without posterior re-magnetization) caused by very large impacts³⁷, could be biased by the strong crustal thinning at large impact places, that would eliminate the major part of magnetisable crustal material and therefore would preclude a substantial re-magnetization at these places, even in presence of a magnetic field³⁶.

I have shown here that Mars also experienced profound changes in its internal dynamics in the same approximate time, including a reduction of heat flow and a drastic increasing of lithosphere strength and thickness. The reduction of heat flow, when compared with global radioactive heat production, indicates a limited cooling (or even a heating-up, consistent with the high temperature of formation of shergottite meteorites) of the deep interior for post-Noachian times. The drastic increasing of lithosphere strength indicates a cold lithosphere (including a strong uppermost mantle and maybe crustal-mantle lithosphere welding) above the inefficiently cooled (or even heated) interior.

The, at least rough, time coincidence of the above mentioned changes (Figure 4) seems unlikely to be accidental. Those changes were most probably linked, suggesting profound interrelations between interior dynamics and environmental evolution of this planet. The reduction of the heat flow from the deep interior produced a cooling and thickening of the lithosphere, evidenced by the drastic increasing in effective elastic thickness deduced for the same approximate time. This in turn would be consistent with a change in magma mineralogy due to a magma source located below a thicker lithosphere.

The rise of mantle temperature caused by an interior heating-up would have reduced the thermal gradient between mantle and core, weakening or even stopping core convection and dynamo^{38,39}. Even if one accepts the earlier chronology for dynamo cessation, it could have been the first sign of the big changes experienced by Mars around the Noachian/Hesperian boundary. The ceasing of the dynamo would eliminate the magnetic shielding of the atmosphere, contributing to their severe erosion, and therefore heavily affecting the climatic and hydrologic evolution of Mars^{31,36}. As a consequence, the erosion/degradation for liquid water would be greatly diminished, and a wetter environment permitting clay formation would transition to more arid conditions favouring the formation of acidic and evaporitic mineralogy.

Low post-Noachian heat flow values could be indicative of an important reduction in mantle convection efficiency, which could in turn be related to inefficient water recycling in a stagnant-lid planet (e.g., Ref. 40). Thus, it is possible that internal water cycles and environmental evolutions were profoundly interrelated throughout the history of Mars. A more profound understanding of these interrelations is necessary for our knowledge of the biological potential of this planet, past, present, or even future.

Methods

Calculation of heat flows from effective elastic thickness. The effective elastic thickness of the lithosphere can be converted to heat flow following the equivalent strength envelope formalism. Here I use an implementation of this methodology which takes into account the strength contributions from the crust and the lithospheric mantle³⁴¹, in order to calculate upper limit heat flows for the Hesperian for Olympus and Arsia Montes, and for the Early Hesperian for Elysium rise. For calculating heat flows I use estimates of both the effective elastic thickness of the lithosphere² and the curvature of the equivalent elastic layer³. I use values widely used for Mars^{1–3} for the Young's modulus (100 GPa), Poisson's ratio (0.25), crustal density (2900 kg m⁻³) and mantle lithosphere density (3500 kg m⁻³). The admittance modeling², from which derive the used effective elastic thicknesses, was performed for a mean crustal thickness of 50 km, whereas the updated crustal thickness map of Neumann *et al.*⁴² was constructed for a mean crustal thickness of 45 km. Thus, in my calculations I assume local crustal thicknesses based on the regional trends of those authors⁴², but increased in 5 km, in order to be consistent with the values of the effective elastic thicknesses: 55, 85 and 45 km for, respectively, Olympus Mons, Arsia Mons, and Elysium rise. For calculating brittle strength I assume zero pore pressure, which serves to put an upper limit to the obtained surface heat flow.

For creep parameters of the Martian crust I use the flow law of wet diabase⁴³, which is consistent with extensive evidence of water-related geological activity in early Mars. The ductile strength of the mantle lithosphere is calculated for dry olivine dislocation creep rheology (a flow law obtained for artificially dried dunites⁴⁴), which give an upper limit to the surface heat flow, which is useful to obtain a lower limit for the Urey ratio. A strain rate of 10⁻¹⁶ s⁻¹ was used in the calculations, based on the faster strain rates in the range usually considered for Mars^{2,3}, which is again useful to obtain a heat flow upper limit; to make a comparison, terrestrial strain rates are typically ~10⁻¹⁶ s⁻¹ in Earth active continental interiors; using slowly strain rates would result in lower heat flows and higher Urey ratios. The base of the mechanical lithosphere is here defined as the depth at which the ductile strength reaches a low value of 10 MPa, and below which there are no further significant increases in strength, although the exact value selected does not produce significant changes in the calculations due to the exponential dependence of ductile strength on temperature. The strength level at the crust base determining if mantle lithosphere and crust are mechanically welded is taken as 10 MPa; again, the exact value selected does not produce significant changes in the obtained results.

For a complete description of this procedure see Ruiz *et al.*⁴¹.

Temperature profiles. I calculate temperature profiles following the procedure described by Ruiz *et al.*³, and using crustal heat-producing elements (HPE) abundances based on Mars Odyssey GRS measurements. The significant homogeneity of elemental abundances measure by Mars Odyssey GRS suggests that the Martian crust is much less geochemically varied than the Earth's crust. Although it is possible that crustal HPE abundances decrease with depth, a homogeneous distribution gives higher surface heat flow and is therefore useful for my upper limit calculations. For the mantle lithosphere I use HPE abundances 0.1 times, per unit mass, the crustal average, consistent with a ratio between crustal and primitive mantle HPE abundances higher than ~10 for Mars. Heat dissipation rates were calculated for standard decay constants.

For the thermal conductivity I use a constant value of 2 W m⁻¹ K⁻¹ for the crust, appropriate for intact (non-porous) basaltic rocks, and a temperature-dependent thermal conductivity appropriate for olivine for the mantle lithosphere. The surface temperature is assumed as 220 K, the present-day mean surface temperature on Mars, which is consistent with the inference of low near-surface temperatures deduced for most of the past 4 Ga from ALH84001 thermochronology⁴⁵.

For a complete explanation and discussion of the values used in the calculations see Ruiz *et al.*³.

Urey ratio calculations. I derive paleo-Urey ratios by calculating the ratio between the total radioactive heat production, for a given time, obtained from the compositional model of Mars of Wänke and Dreibus¹⁷ and standard decay constants, and the surface heat flow derived from lithospheric strength. Thus, the paleo-Urey ratio is given by $H(\text{age}) M_{\text{mars}} / (4\pi R_{\text{mars}} F)$, where $H(\text{age})$ is the mean heat production rate by mass unit, M_{mars} and R_{mars} are, respectively, the mass and the mean radius of Mars, and F is the surface heat flows derived for a given feature and age. The so-derived Ur values are in fact "equivalent" Ur values, since they are based on "local" paleo-heat flows.

Ranges of effective elastic thickness of the lithosphere. Values of effective elastic thickness have been compiled from literature^{2,18,20,26,27,46–55}. In the case of features for



which two or more different T_e ranges have been proposed (as is the case for the Tharsis volcanoes) I have consigned the range of elastic thicknesses consistent with all the estimates, which are therefore considered equally valid.

- Zuber, M. T. *et al.* Internal structure and early thermal evolution of Mars from Mars Global Surveyor. *Science* **287**, 1788–1793 (2000).
- McGovern, P. J. *et al.* Correction to Localized gravity/topography admittance and correlation spectra on Mars: implications for regional and global evolution. *J. Geophys. Res.* **109**, E07007; DOI:10.1029/2004JE002286 (2004).
- Ruiz, J. *et al.* 2011. The thermal evolution of Mars as constrained by paleo-heat flows. *Icarus* **215**, 508–517 (2011).
- Hauck, S. A. & Phillips, R. J. Thermal and crustal evolution of Mars. *J. Geophys. Res.* **107**, 5052; DOI:10.1029/2001JE001801 (2002).
- Grott, M. & Breuer, D. On the spatial variability of the martian elastic lithosphere thickness: evidence for mantle plumes? *J. Geophys. Res.* **115**, E03005; DOI:10.1029/2009JE003456 (2010).
- Fraeman, A. A. & Korenaga, J. The influence of mantle melting on the evolution of Mars. *Icarus* **210**, 43–57 (2010).
- Yoder, C. F., Konopliv, A. S., Yuan, D. N., Standish, E. M. & Folkner, W. M. Fluid core size of Mars from detection of the solar core. *Science* **300**, 299–303 (2003).
- Acuña, M. H. *et al.* Magnetic field of Mars: summary of results from the aerobraking and mapping orbits. *J. Geophys. Res.* **106**, 23,403–23,417 (2001).
- Nahm, A. L. & Schultz, R. A. Magnitude of global contraction on Mars from analysis of surface faults: implications for Martian thermal history. *Icarus* **211**, 389–400 (2011).
- Hauber, E., Broz, P., Jagert, F., Jodlowski, F. & Platz, T. Very recent and widespread basaltic volcanism on Mars. *Geophys. Res. Lett.* **38**, L10201; DOI:10.1029/2011GL047310 (2011).
- Ruedas, T., Tackley, P. J. & Solomon, S. C. Thermal and compositional evolution of the martian mantle: effects of phase transitions and melting. *Phys. Earth Planet. Inter.* **216**, 32–58 (2013).
- Musselwhite, D. S., Dalton, H. A., Kiefer, W. S. & Treiman, A. H. Experimental petrology of the basaltic shergottite Yamato-980459: implications for the thermal structure of the Martian mantle. *Meteor. Planet. Sci.* **41**, 1271–1290 (2006).
- Collinet, M., Médard, E., Devouard, B. & Peslier, A. Constraints on the parental melts of enriched shergottites from image analysis and high pressure experiments. *Lunar Planet. Sci. Conf.* **43**, 2269 (2012).
- Filiberto, J. & Dasgupta, R. Constraints on the depths and thermal vigor of basalt formation in the martian mantle. Paper presented at *The Mantle of Mars: Insights from Theory, Geophysics, High-Pressure Studies, and Meteorites*, Houston. LPI Contribution 1684–6019 (2012, September 10–12).
- Hartmann, W. K. & Neukum, G. Cratering chronology and the evolution of Mars. *Space Sci. Rev.* **96**, 165–194 (2001).
- Wänke, H. & Dreibus, G. Chemical composition and accretion history of terrestrial planets. *Phil. Trans. R. Soc. London A* **325**, 545–557 (1988).
- Werner, S. C. The global martian volcanic evolutionary history. *Icarus* **201**, 44–68 (2009).
- Beuthe, M., Le Maistre, S., Rosenblatt, P., Pätzold, M. & Dehant, V. Density and lithospheric thickness at the Tharsis Province from MEX MaRS and MRO gravity data. *J. Geophys. Res.* **117**, E04002; DOI:10.1029/2011JE003976 (2012).
- Isherwood, J., Jozwiak, L. M., Jansen, J. C. & Andrews-Hanna, J. C. The volcanic history of Olympus Mons from paleo-topography and flexural modeling. *Earth Planet. Sci. Lett.* **363**, 88–96, 2013.
- Ruiz, J. *et al.* Ancient heat flow, crustal thickness, and lithospheric mantle rheology in the Amenthes region, Mars. *Earth and Planetary Science Letters* **270**, 1–12 (2008).
- Grott, M., Hauber, E., Werner, S. C., Kronberg, P. & Neukum, G. Mechanical modelling of thrust faults in the Thaumasia region, Mars, and implications for the Noachian heat flux. *Icarus* **186**, 517–526 (2007).
- Watts, A. B. & Burov, E. B. Lithospheric strength and its relation to the elastic and seismogenic layer thickness. *Earth Planet. Sci. Lett.* **213**, 113–131 (2003).
- Williams, J.-P., Ruiz, J., Rosenburg, M. A., Aharonson, O. & Phillips, R. J. Solar insolation driven variations of Mercury's lithospheric strength. *J. Geophys. Res.* **116**, E01008; DOI:10.1029/2010JE003655 (2011).
- Grott, M. & Breuer, D. The evolution of the martian elastic lithosphere and implications for crustal and mantle rheology. *Icarus* **193**, 503–515 (2008).
- Grott, M. *et al.* Long-term evolution of the martian crust-mantle system. *Space Sci. Rev.* **174**, 49–111 (2013).
- Phillips, R. J. *et al.* Mars north polar deposits: stratigraphy, age, and geodynamical response. *Science* **320**, 1182–1185 (2008).
- Wieczorek, M. A. Constraints on the composition of the martian south polar cap from gravity and topography. *Icarus* **196**, 506–517 (2008).
- Carr, M. H. & Head, J. W. Geologic history of Mars. *Earth Planet. Sci. Lett.* **294**, 185–203 (2010).
- Fassett, C. I. & Head, J. W. Sequence and timing of conditions on early Mars The timing of martian valley network activity: constraints from buffered crater counting. *Icarus* **211**, 1204–1214 (2011).
- Mangold, N., Adeli, S., Conway, S., Ansan, V. & Langlais, B. A chronology of early Mars climatic evolution from impact crater degradation. *J. Geophys. Res.* **117**, E04003; DOI:10.1029/2011JE004005 (2012).
- Bibring, J. P. *et al.* Global mineralogical and aqueous Mars history derived from OMEGA/Mars express data. *Science* **312**, 400–404 (2006).
- Ehlmann, B. L. *et al.* Subsurface water and clay mineral formation during the early history of Mars. *Nature* **479**, 53–60 (2011).
- Baratoux, D., Toplis, M. J., Monnereau, M. & Sautter, V. The petrological expression of early Mars volcanism. *J. Geophys. Res.* **118**, 59–64 (2013).
- Wilson, J. H. & Mustard, J. F. Exposures of olivine-rich rocks in the vicinity of Ares Vallis: implications for Noachian and Hesperian volcanism. *J. Geophys. Res.* **118**, 916–929 (2013).
- Milbury, C., Schubert, G., Raymond, C. A., Smrekar, S. E. & Langlais, B. The history of Mars' dynamo as revealed by modelling magnetic anomalies near Tyrrhenus Mons and Syrtis Major. *J. Geophys. Res.* **117**, E10007; DOI:10.1029/2011JE004005 (2012).
- Langlais, B., Thébaud, E. Y., Quesnel, Y. & Mangold, N. A Late Martian Dynamo Cessation Time 3.77 Gy Ago. *Lunar Planet. Sci. Conf.* **43**, 1231 (2012).
- Lillis, R. J., Robbins, S., Manga, M., Halekas, J. S. & Frey, H. V. Time history of the Martian dynamo from crater magnetic field analysis. *J. Geophys. Res.* **118**, DOI:10.1002/jgre.20105 (2013).
- Nimmo, F. & Stevenson, D. J. Influence of early plate tectonics on the thermal evolution and magnetic field of Mars. *J. Geophys. Res.* **105**, 11,969–11,979 (2000).
- Breuer, D. & Spohn, T. Early plate tectonics versus single-plate tectonics on Mars: Evidence from magnetic field history and crust evolution. *J. Geophys. Res.* **108**, 5072; DOI:10.1029/2002JE001999 (2003).
- Sandu, C. & Kiefer, W. S. Degassing history of Mars and the lifespan of its magnetic dynamo. *Geophys. Res. Lett.* **39**, L03201; DOI:10.1029/2011GL050225 (2012).
- Ruiz, J., Gómez-Ortiz, D. & Tejero, R. Effective elastic thicknesses of the lithosphere in the Central Iberian Peninsula from heat flow: implications for the rheology of the continental lithospheric mantle. *J. Geodyn.* **41**, 500–509 (2006).
- Neumann, G. A., Lemoine, F. G., Smith, D. E. & Zuber, M. T. Marscrust3-A crustal thickness inversion from recent MRO gravity solutions. *Lunar Planet. Sci. Conf.* **39**, 2167 (2008).
- Caristan, Y. The transitions from high temperature creep to fracture in Maryland diabase. *J. Geophys. Res.* **87**, 6781–6790 (1982).
- Chopra, P. N. & Paterson, M. S. The role of water in the deformation of dunite. *J. Geophys. Res.* **89**, 7861–7876 (1984).
- Shuster, D. L. & Weiss, B. P. Martian surface paleotemperatures from thermochronology of meteorites. *Science* **309**, 594–597 (2005).
- Kiefer, W. S. Gravity evidence for an ancient extinct magma chamber beneath Syrtis Major, Mars: a look at the magmatic plumbing system. *Earth Planet. Sci. Lett.* **222**, 349–361 (2004).
- Kiefer, W. S. Buried mass anomalies along the hemispheric dichotomy in eastern Mars: implications for the origin and evolution of the dichotomy. *Geophys. Res. Lett.* **32**, L22201; DOI:10.1029/2005GL024260 (2005).
- Bellengui, V., lognonné, P. & Wieczorek, M. Constraints on the martian lithosphere from gravity and topography data. *J. Geophys. Res.* **110**, E11005; DOI:10.1029/2005JE002437 (2005).
- Grott, M., Hauber, E., Werner, S. C., Kronberg, P. & Neukum, G. High heat flux on recent Mars: Evidence from rift flank uplift at Coracis Fossae. *Geophys. Res. Lett.* **32**, L21201; DOI:10.1029/2005GL023894 (2005).
- Hoogenboom, T. & Smrekar, S. E. Elastic thickness estimates for the northern lowlands of Mars. *Earth Planet. Sci. Lett.* **248**, 830–839 (2006).
- Kronberg, P. *et al.* Acheron Fossae, Mars: tectonic rifting, volcanism, and implications for lithospheric thickness. *J. Geophys. Res.* **112**, E04005; DOI:10.1029/2006JE002780 (2007).
- Milbury, C. A. E., Smrekar, S. E., Raymond, C. A. & Schubert, G. Lithospheric structure in the eastern region of Mars' dichotomy boundary. *Planet. Spa. Sci.* **55**, 280–288 (2007).
- Williams, J.-P., Nimmo, F., Moore, W. B. & Paige, D. A. The formation of Tharsis on Mars: what the line-of-sight gravity is telling us. *J. Geophys. Res.* **113**, E10011; DOI:10.1029/2007JE003050 (2008).
- Ritzler, J. A. & Hauck, S. A. Lithospheric structure and tectonic at Isidis Planitia, Mars. *Icarus* **201**, 528–539 (2009).
- Grott, M. & Wieczorek, M. A. Density and lithospheric structure at Tyrrhena Patera, Mars, from gravity and topography data. *Icarus* **221**, 43–52 (2012).
- Tanaka, K. L. The stratigraphy of Mars. *J. Geophys. Res.* **91**, E139–E158 (1986).
- Frey, H. V. Impact constraints on, and a chronology for, major events in early Mars history. *J. Geophys. Res.* **111**, E08S91; DOI:10.1029/2005JE002449 (2006).
- Fristad, K. E. & Frey, H. V. Age variations in the martian lowlands. *Lunar Planet. Sci. Conf.* **37**, 1406 (2006).
- Werner, S. C. The early martian evolution-constraints from basin formation age. *Icarus* **195**, 45–60 (2008).
- Platz, T., Michael, G., Tanaka, K. L., Skinner, J. A. & Fortezzo, C. M. Crater-based dating of geological units on Mars: methods and application for the new global geological map. *Icarus* **225**, 806–827 (2013).

Acknowledgments

I thank Valle Lopez for logistical help. I also thank Katherine Bramble for English improvement of this manuscript. The author is an employee at the Universidad



Complutense with a contract Ramón y Cajal co-financed from the Ministerio de Ciencia e Innovación of Spain and the European Social Fund (ESF).

Author contributions

J.R. is the only author of this work.

Additional information

Competing financial interests: The authors declare no competing financial interests.

How to cite this article: Ruiz, J. The early heat loss evolution of Mars and their implications for internal and environmental history. *Sci. Rep.* 4, 4338; DOI:10.1038/srep04338 (2014).



This work is licensed under a Creative Commons Attribution-NonCommercial-NoDerivs 3.0 Unported license. To view a copy of this license, visit <http://creativecommons.org/licenses/by-nc-nd/3.0>